

Copyright 2008 Society of Photo-Optical Instrumentation Engineers.

This paper was (will be) published in Proc. SPIE 7013 and is made available as an electronic reprint (preprint) with permission of SPIE. One print or electronic copy may be made for personal use only. Systematic or multiple reproduction, distribution to multiple locations via electronic or other means, duplication of any material in this paper for a fee or for commercial purposes, or modification of the content of the paper are prohibited.

Fringe tracking and spatial filtering: phase jumps and dropouts

David F. Buscher, John S. Young, Fabien Baron, Christopher A. Haniff
Cavendish Laboratory, J. J. Thomson Avenue, Cambridge CB3 0HE, U.K.

ABSTRACT

Fringe tracking in interferometers is typically analyzed with the implicit assumption that there is a single phase associated with each telescope in the array. If the telescopes have apertures significantly larger than r_0 and only partial adaptive optics correction, then the phase measured by a fringe sensor may differ significantly from the “piston” component of the aperture phase. In some cases, speckle noise will cause “branch points” in the measured phase as a function of time, causing large and sudden jumps in the phase. We present simulations showing these effects in order to understand their implications for the design of fringe tracking algorithms.

1. INTRODUCTION

A central component of any separated-element interferometer is the system which tracks and corrects the time-varying phase differences between different apertures in the interferometer. Typically, these systems are called “fringe trackers” because they measure the phase of an interference fringe pattern, and they measure and correct only one spatial degree of freedom per aperture. This degree of freedom is commonly assumed to be simply the “piston” mode of the wavefront error across the aperture, corresponding to the average wavefront error, and the correction is applied using an actuator capable of introducing piston, for example a delay line.

Fringe-tracking systems have been operated successfully in interferometers such as the Mark III interferometer¹ and PTI,² and indeed were critical to their scientific success. Both these interferometers had apertures which were small compared with r_0 at the operating wavelength, and this means that the approximation that there was only one atmospheric spatial phase perturbation associated with each aperture was justifiable. The latest generation of arrays such as CHARA,³ Keck Interferometer⁴ and VLTI,⁵ all have apertures which are much larger than r_0 , and so it is important to consider what the effects might be of having significant (>1 radian) perturbations across the apertures of each telescope.

Earlier investigations by Tubbs^{6,7} showed that, in multi- r_0 interferometers with beam combiners incorporating spatial filters, the interaction between the focal plane “speckles” and the spatial filter gave rise to substantial differences between the piston component of the wavefronts and the phase of the wavefront transmitted through a spatial filter. Studies by G. Daigne (private communication) showed that the combination of spatial wavefront errors and diffraction effects in the interferometric beam train could give rise to substantial phase anomalies between the piston phase and the phase as measured in an interference fringe.

Here we tackle the question as to how and why spatial wavefront corrugations can give rise to differences between the piston phase and the phase measured by a beam combiner. We show that these effects are quite general to all multi- r_0 interferometers and can arise whether or not diffraction or spatial filtering are present in the instrumental setup. We investigate briefly how spatial filtering and adaptive optics affect the character of these phase anomalies, in order to understand how best to design interferometers and their associated fringe-tracking systems.

D.F.B.: E-mail: dfb@mrao.cam.ac.uk, Telephone: +44 (0)1223 337302

2. MEASUREMENT MODEL

We adopt here a simple model of an interferometer which is nevertheless capable of exhibiting the effects of spatial perturbations. The interferometer consists of two telescopes with circular apertures of diameter D observing a distant unresolved source. The stellar wavefronts pass through an atmospheric phase screen containing Kolmogorov-Tatarski spatial phase perturbations with Fried parameter r_0 , and the phase screen is assumed to evolve with time as predicted by the Taylor hypothesis, with a single phase screen moving at velocity \mathbf{v} across the apertures — more complex models with multiple layers moving in different directions were not considered here. The apertures are modeled as being sufficiently far apart that the phase screens over each aperture are uncorrelated, but that the wind velocity and direction are the same for both apertures.

The telescopes each have an adaptive optics (AO) system. The AO is modeled as a perfect modal filter, which is to say that the first n Zernike modes (excluding piston) are removed from the wavefront. Values of n from 2 to 20 are considered here, where case $n = 2$ corresponds to a tip/tilt correction system while $n = 20$ corresponds to a fifth-radial-order system.

The wavefronts from the telescopes are modeled as propagating without diffraction or further degradation to a fringe-tracking sensor. For the purposes of this paper, the sensor is modeled as a beam combiner which makes a quasi-monochromatic fringe pattern and uses the phase of the detected fringes as a measure of the piston difference between the two telescopes. Phase changes of more than one wavelength are assumed to be tracked using “phase unwrapping” techniques, i.e. following the phase evolution with time and resolving any 2π ambiguities in the phase by assuming that the phase changes are continuous with time. We make no attempt here to model beam combiners with multiple spectral channels or using envelope or group-delay tracking methods, but we consider the implications of such methods in the discussion.

Two sorts of beam combiner are considered. For an “unfiltered” combiner, the wavefronts from the two telescopes are overlapped in either the pupil or the image plane, and fringes are detected either through spatial and/or temporal modulation of the fringes. All the light collected by the telescopes is detected: no spatial filtering takes place.

In a “spatially filtered” combiner, the wavefront is subject to spatial filtering either before or after beam combination (we assume that the spatial filter is identical for both beams, so whether filtering occurs before or after combination makes no difference to the resulting signal). Two forms of spatial filtering are modeled: in “pinhole” spatial filtering we assume that a pinhole is placed in a focal plane somewhere in the optical system, so that only light from the central speckle can pass through. The diameter of the pinhole is assumed to be much less than λ/D where λ is the wavelength of the radiation being observed (in practice a pinhole diameter which is approximately λ/D is to be preferred at low light levels,⁸ but the approximation of an infinitely small pinhole used here simplifies the mathematics considerably).

In “fiber” spatial filtering, we assume a single-mode fiber or other mono-mode waveguide is used to spatially filter the wavefront. The mode accepted by the filter is assumed to be Gaussian-shaped and the f-ratio of the optical system coupling the light from the aperture into the waveguide is assumed to be such that the diameter of the contour of the far-field mode profile where the mode amplitude drops to $1/e$ of the peak amplitude is 0.9 times the aperture diameter, corresponding to optimal coupling to the aperture.⁹

Fringe detection is assumed to be noiseless, i.e. the source is bright so there is no detector or photon noise, so that any errors in the measured phase arise purely from atmospheric distortions.

3. SIMPLIFIED ANALYSIS

In this section we attempt to gain some insight into what is measured by an idealized fringe sensor and why and under what circumstances this differs from the piston component of the wavefront. We consider only the unfiltered combiner and the pinhole-filtered combiner, since analysis of the fiber-filtered combiner is more complex and does not yield any qualitatively new insights.

If we consider the fringes formed by an unfiltered beam combiner (whether pupil-plane or image-plane), it is straightforward to show¹⁰ that the measured fringe pattern can be characterized by a complex fringe amplitude

given by

$$A = \int_S e^{i[\phi_1(\mathbf{x}) - \phi_2(\mathbf{x})]} dS \quad (1)$$

where $\phi_1(\mathbf{x})$ and $\phi_2(\mathbf{x})$ are the phase perturbations at position \mathbf{x} within apertures 1 and 2 respectively (we define the coordinate systems separately for the two apertures such that the value of \mathbf{x} represents the position with respect to the center of the relevant aperture), dS is an elemental within the aperture and the integral over S denotes integrating over the clear area of the aperture. It is similarly straightforward to show that, for a filtered combiner, the measured fringe complex amplitude is given by

$$A = A_1 A_2^* \quad (2)$$

where A_1 is the complex amplitude of the beam from aperture 1 after it has been spatially filtered. In the case of an infinitely small pinhole spatial filter A_1 is given by:

$$A_1 = \int_S e^{i\phi_1(\mathbf{x})} dS, \quad (3)$$

so that

$$A = \int_S e^{i\phi_1(\mathbf{x})} dS \int_S e^{-i\phi_2(\mathbf{x})} dS \quad (4)$$

In both the filtered and unfiltered cases the measured phase will be the argument of the measured complex fringe amplitude A . We can compare this with the expression for the piston component of the wavefront across each of the apertures. The piston component of the phase across aperture 1 will be given by:

$$\Phi_1 = \int_S \phi_1(\mathbf{x}) dS \quad (5)$$

and the piston difference between the apertures will be given by

$$\Phi = \Phi_1 - \Phi_2 = \int_S \phi_1(\mathbf{x}) - \phi_2(\mathbf{x}) dS \quad (6)$$

It is readily apparent that, while there is some similarity between, for example, equation 6 and the phase of the complex amplitude given in equation 1, it is by no means obvious that they should in general give the same answer.

However, it is clear that they do measure the same quantity in the limit of no phase fluctuation across the aperture, and it is also possible to derive the relationship between the two for the case when there are only small amounts of phase perturbations. If the phase is approximately constant across the aperture such that

$$\phi_1(x) = \phi_1 + \delta\phi_1(\mathbf{x}) \quad (7)$$

$$\phi_2(x) = \phi_2 + \delta\phi_2(\mathbf{x}) \quad (8)$$

where $\delta\phi_1(\mathbf{x}) \ll 1$ and $\delta\phi_2(\mathbf{x}) \ll 1$, then we can do a Taylor expansion of the complex exponentials in the above expressions. For example, we can derive from equation 3 that

$$A_1 \approx e^{i\phi_1} \left[1 - \frac{1}{2} \int_S \{\delta\phi_1(\mathbf{x})\}^2 dS + i \int_S \delta\phi_1(\mathbf{x}) dS - \frac{i}{6} \int_S \{\delta\phi_1(\mathbf{x})\}^3 dS \right] \quad (9)$$

and by considering the real and imaginary components of the term in the square brackets, we can see that the phase of this quantity is given approximately by

$$\arg(A_1) \approx \phi_1 + \frac{\int_S \delta\phi_1(\mathbf{x}) dS - \frac{1}{6} \int_S \{\delta\phi_1(\mathbf{x})\}^3 dS}{1 - \frac{1}{2} \int_S \{\delta\phi_1(\mathbf{x})\}^2 dS} \quad (10)$$

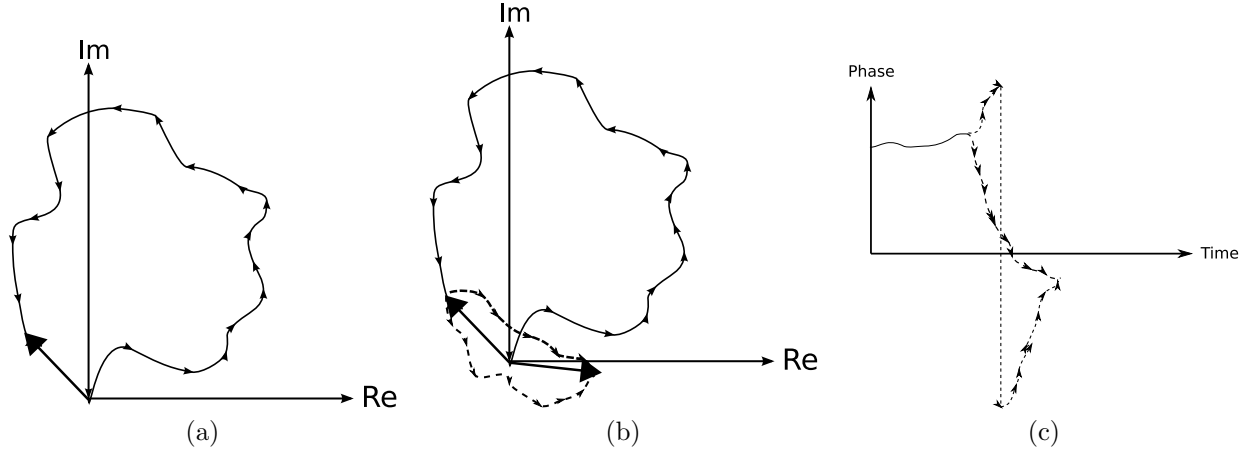


Figure 1. (a) A complex amplitude summation in the complex plane, showing a low amplitude resultant phasor (b) Two possible subsequent evolution paths (shown as dotted lines) ending up at the same resultant phasor (c) The corresponding phase evolution showing a phase “branch point”. The principal value of the phase is plotted, i.e. the phase jumps between $+\pi$ and $-\pi$ to keep the value within range.

We can see that, to first order in $\delta\phi_1$, the phase of A_1 is indeed equal to the piston phase. Furthermore, the deviation between the piston phase and the argument of the complex amplitude will scale approximately as $\delta\phi^3$.

We can derive similar results for the phases of the filtered and unfiltered fringes, namely that the fringe phase accurately represents the piston phase when the instantaneous phase fluctuations across the aperture are small when compared to a radian, but that as the phase fluctuations approach a radian, there will be a rapid divergence between the piston phase and the measured fringe phase.

When the aperture phase deviations $\delta\phi$ become large compared to a radian, it is possible for large divergences between the fringe phase and the piston phase to appear. What is more, these divergences can give rise to behavior which can be termed chaotic, by which we mean that relatively small changes in the distribution of phase values in the aperture can give rise to large differences in the final outcome.

To see this, let us consider the wavefront across an aperture at two instants in time, which are separated by an interval which is small compared to D/v , the time taken for the wind to sweep the phase screen across the aperture. At any one instant we can treat the integral across the aperture in equation 3 as the limit of a sum of phasors in the complex plane. If the range of phase values is large compared to a radian, we can end up with the resulting sum being of small amplitude, i.e. close to the origin of the complex plane as shown in Figure 1(a).

The low modulus corresponds to an instant of low Strehl ratio in the focal plane image, but at the same time corresponds to a regime of extreme sensitivity of the phase to small perturbations. For example, at a time $\Delta t \ll D/v$ later, the distribution of phases across the aperture will have changed by only a small amount: if the Taylor hypothesis holds, approximately $1 - \Delta t v/D$ of phasors will be identical and only the fraction $v\Delta t/D$ of the phasors will be different. If we track this small change in time, then two possible evolutionary paths are shown Figure 1(b). It can be seen that two small and nearly identical evolutionary histories for the aperture phases give two very different tracks in the fringe phase as shown in Figure 1(c), despite the fact that the piston phase ends up at the same point.

We can see from this example that it is possible under conditions of large phase perturbations to generate rapid “jumps” in the fringe phase which are not seen in the piston phase. Furthermore, these jumps can cause a 2π “wrap around” in the fringe phase which will confuse any “phase unwrapping” algorithm in a similar to the phase “branch points” seen in 2-D phase maps.

In summary then, we have shown that the piston phase and fringe phase will track each other closely if the instantaneous phase perturbations across the aperture are small compared with a radian, but that large differences can appear as the fluctuations approach and exceed a radian.

4. SIMULATIONS

4.1 Simulation method

In order to demonstrate these effects numerically, a computer simulation of the interferometer model was set up. Kolmogorov-Tatarski phase screens were generated on a regular grid by Fourier-transforming filtered white noise.¹⁰ The grid sampled the phase at intervals of $r_0/6$ or less and the grid extent was typically greater than $160r_0$. Time series of Taylor screens were generated by “sliding” the telescope aperture across the phase screen, interpolating the phase screen onto a regular grid in the aperture plane. It was possible to generate long non-repeating sequences of aperture phase snapshots by setting the “wind” velocity vector at 30° to the grid axes and “wrapping” round when the aperture reached the edge of the phase screen (this makes use of the cyclic edge-to-edge continuity of the Fourier-generated phase screens). Statistically independent phase screens were used for each of the apertures.

Adaptive optics was simulated by projecting out Zernike modes from the aperture phases and subtracting these modes. Three different beam combiners were simulated: an unfiltered beam combiner, a pinhole combiner (with an infinitely small pinhole) and a fiber combiner. Time series of the complex fringe amplitudes measured by these combiners were generated, together with, in the case of the filtered combiners, the complex amplitudes of each of the filtered beams. The piston phase for each aperture was calculated as well as a modified version of the piston phase with a Gaussian weighting across the aperture. The latter was used as a comparison with the fiber-filtered fringe data, so that effects due to the aperture weighting of the fiber could be eliminated, i.e. at small D/r_0 this modified piston phase and the fiber phase should converge rapidly to one another.

4.2 Phase jumps

Figure 2 shows the output of one of the simulations. It shows a system with $D/r_0 = 4$ and tip/tilt correction, where the mean Strehl ratio is greater than 0.3. Nevertheless, the Strehl ratio shows frequent “dropouts” to much lower values; this is due only to the statistical nature of the phase fluctuations as a perfect tip/tilt system has been modeled.

For most of the time, the fringe phase tracks the piston phase to much better than a radian, but on some (but not all) of the occasions where the Strehl in one aperture or another falls to a low value, the phase measured by the beam combiner shows large “jumps” where the measured phase differs from the piston phase by more than a radian. These jumps are fast: the time axis is plotted in units of r_0/v , and so for $D/r_0 = 4$ we see that, as expected from “aperture filtering”, the piston phase shows no structure on timescales of less than 4 units, while the phase jumps occur on timescales of 1-2 units.

This observation follows what is expected from the previous analysis: when the Strehl is low, the measured phase can change rapidly and by large amounts. Note that the Strehl being low does not inevitably lead to large phase jumps, since the combination of low Strehl and a suitable subsequent evolution of the aperture phase distribution are needed to cause large phase fluctuations.

The combination of low Strehl and fast fluctuations represents a double challenge for a fringe tracker, because the low Strehl ratio implies that the signal-to-noise ratio on a fringe measurement is reduced. At the same time, the phase is changing rapidly, so the tracker must sample fast to keep up. Even if the tracker is able to meet these stringent requirements, we can see that it will still perform less than adequately on some occasions: in the first large jump in phase seen in Figure 2, we can see that the phase difference between the fringe-tracker phase and the piston phase wraps through 2π radians (i.e. we have gone through a “branch point”), so the fringe tracker will end up one fringe off the fringe it was initially following. If these jumps continue, the tracker could eventually end up losing the fringe packet altogether.

The frequency of such large jumps depends on the D/r_0 value for the aperture. At $D/r_0 = 4$ such jumps are seen in almost every sequence of the length shown in Figure 2: for typical values at visible wavelengths of $r_0 = 10\text{cm}$ and $v = 10\text{m/s}$ this correspond to timescales of order 1 second. For lower D/r_0 values, the rate of such jumps fall dramatically, such that at $D/r_0 = 3$ much longer sequences are required to see the jumps. A statistical analysis of the rate of these jumps as a function of aperture size will be the subject of a later paper.

It might be argued that the fact that the fringe tracker does not follow the “piston phase” is irrelevant, because what is important that we follow the phase seen by the science camera. However, if the science camera is at

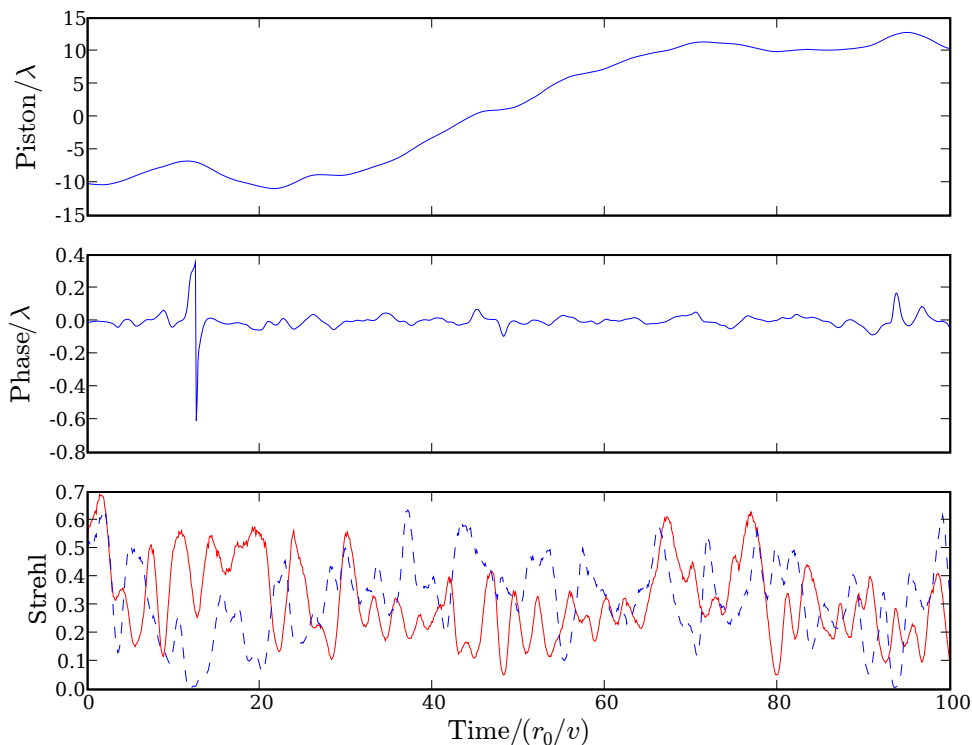


Figure 2. Simulated time-sequences for an interferometer with tip/tilt correction and $D/r_0 = 4$. The top graph shows the measured piston phase, which shows the smoothing expected from “aperture filtering”. Below it is the difference between the piston phase and the phase measured with a fiber-filtered beam combiner. The bottom graph shows the Strehl ratios seen at each of the two telescopes, shown as solid and dashed lines respectively. It can be seen that there are occasional large phase “jumps” associated with periods of low Strehl.

a different wavelength to the fringe tracker, then due to the non-linear nature of the phase jump phenomenon, the phase jumps seen in the science camera and the fringe tracker are only weakly correlated. Figure 3 shows a simulation where the wavelength ratio between the science camera and fringe tracker is only 1.5 (it does not matter which way round the ratio is for the purposes of this analysis), and yet the phase jumps seen at one wavelength are rarely mimicked at the other wavelength.

4.3 Spatial filtering

An interesting question to ask is whether or not spatial filtering improves or makes worse the differences between the piston phase and the measured phase. The implication from Tubbs’ work⁷ was that spatial filtering might in fact be the source of the anomalies, but we have already shown that this is not the case.

As we have seen, the phase anomalies are associated with non-linear effects which occur when the the variation of the phase of the complex exponentials in equations 1 and 4 become comparable to a radian. It can be readily shown that the instantaneous variation of the imaginary argument to the exponential for the unfiltered combiner (equation 1) will typically be larger by a factor of order $\sqrt{2}$ than that for the for the filtered combiner (equation 4), and therefore we expect the unfiltered combiner to be *more* likely to be affected by phase anomalies than the filtered combiner: phase jumps correspond to the infrequent realizations in the “tail” of the set of possible instantaneous aperture phase distributions, and the chance of the instantaneous fluctuations approaching or exceeding a radian is significantly greater for the unfiltered combiner. The fact that there are two “chances” (one for each integral in equation 4) to have an unusual distribution in the case of the filtered combiner does not make up for the greater probability of a large-variance event in the unfiltered combiner.

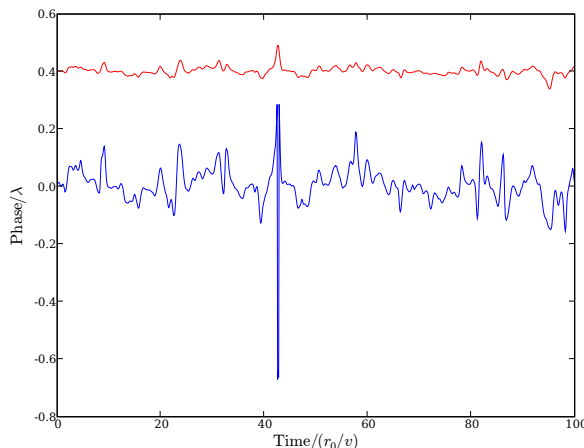


Figure 3. Simulated phase sequences seen in two beam combiners operating at different wavelengths. The upper sequence (offset for clarity) is for a combiner operating at a D/r_0 value of 3, while the lower sequence is for a wavelength a factor of 1.5 times smaller. We can see that the magnitude of the phase jumps at different wavelengths rarely if ever exhibit the ideal ratio of 1.5 and hence fringe tracking at one wavelength will not perfectly track the phase jumps at another wavelength. The system has tip/tilt correction only.

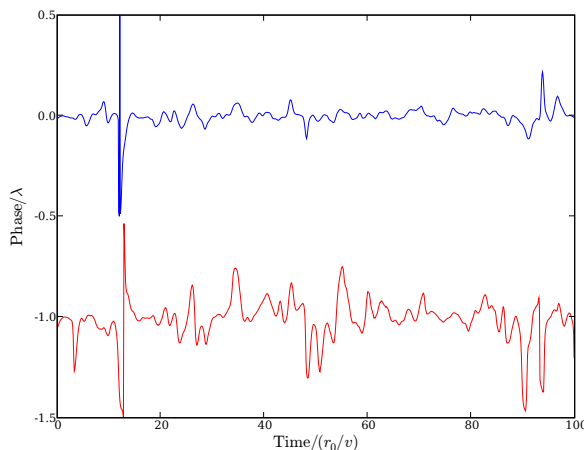


Figure 4. A comparison of the phases measured by a pinhole-filtered beam combiner (top) and an unfiltered beam combiner (bottom), made using the same wavefronts. The simulated value of D/r_0 is 4, and the system is tip/tilt corrected.

The simulation bears out this analysis: Figure 4 shows that the phase jumps are both larger and more frequent in the unfiltered combiner than in the filtered combiner.

4.4 The effect of adaptive optics

The analysis presented earlier indicates that it is the size of the spatial fluctuations that determines the strength of the anomalies seen between the phase measured by a fringe sensor and the piston phase. A higher-order AO system operating on a given aperture size will therefore reduce the likelihood of seeing phase anomalies. However, AO systems are typically sized to the aperture they will be used on, so a more interesting question is whether a large aperture system with high-order AO is better than a small-aperture system with lower-order AO.

To first order, we expect that the AO system will be designed to give a certain minimum Strehl ratio for the aperture/science wavelength combination it is being used with. Given that the Strehl is a monotonic function of the RMS residual phase perturbations in the aperture, we might expect apertures with different orders of AO

but the same Strehl to show similar phase-tracking anomalies. In fact, the simulations do not bear this out: the mean Strehl ratio at which higher-order AO systems first exhibit frequent phase anomalies appears to be lower than for their lower-order counterparts.

One possible explanation lies in the spatial structure of the residual phases: seen in the image plane, a higher-order system of the same Strehl ratio will have a higher contrast between the central speckle and the speckle “halo”. Examination of simulated image data at the moments when the large phase jumps are seen shows that these occur when the central speckle disappears and gives its energy to a new speckle. The tip/tilt component of the AO system will tend to recenter on the new speckle, making it the central speckle, which, at least in a spatially-filtered system, then dominates the phase of the fringes. This new speckle will have a completely different phase from the original central speckle and therefore give rise to a rapid jump in the measured phase. The theory as to why higher-order systems are better would then have to invoke the fact that such a “speckle exchange” event is far more unlikely in the higher-order case, because the chance of one of the subsidiary speckles having comparable energy to the main speckle is finite. This needs to be investigated further to determine if this theory provides a consistent explanation for all the phenomena observed.

5. DISCUSSION AND CONCLUSIONS

We have seen that discrepancies can arise between the phase measured by a fringe sensor and the piston phase, and that these are a strong function of the level of phase corrugations across the aperture. These discrepancies are often seen in the form of large and rapid phase “jumps” and they occur preferentially when the instantaneous Strehl ratio or the fringe amplitude is small, making these jumps hard for the fringe tracker to follow. Indeed, if the fringe tracker does follow these excursions, it may be doing the wrong thing, either because it will “phase wrap” onto the wrong fringe, and/or will follow a phase excursion which is not seen at the science wavelength.

Both spatial filtering and adaptive optics help to reduce the level of such anomalies, but do not eliminate them. The only way to completely avoid these anomalies is to work in a regime where these jumps are unlikely, by selecting appropriate values for D/r_0 and the spatial order of the AO system. In practice this is quite difficult to do: while it is possible to adjust the effective aperture of the system appropriate to the prevailing value of r_0 using a simple diaphragm, there are two problems with this approach. Firstly, for most AO systems it is difficult to change the effective aperture size dynamically and still maintain the same spatial order of correction, because this involves rescaling the spatial resolution of both the wavefront sensor and the wavefront corrector to the new aperture size. Secondly, it is quite difficult to maintain an optimum aperture size because of rapid variations in the seeing. Measurements by Baldwin *et al.*¹¹ show that, at least on one (quite good) site and at some times, the spatial scale of the seeing can vary by factors of more than 2 on timescales of a few hundred milliseconds as shown in Figure 5.

The above arguments suggest that all successful fringe trackers need to be able to deal with rapid phase jumps. This requires development of robust fringe-tracking algorithms which either recognize the phase jumps when they occur (perhaps this may be possible using auxiliary data from the AO system?), or recover rapidly from the loss of fringe lock that may result. An alternative is to use algorithms that are inherently insensitive to rapid phase variations. An example is group-delay fringe tracking or any similar algorithm which tracks the coherence envelope of the fringes rather than the fringe phase. These algorithms tend to average the data over timescales of many tens of t_0 , so that infrequent and rapid anomalies in the phase will have little effect. These algorithms have the additional advantage that they are little affected by short periods of poor seeing. However, the investigation here has only been the effects on a phase-tracking system and not a group-delay system, and so this is a fruitful area for future research.

6. ACKNOWLEDGMENTS

Our search for perfection in fringe tracking received considerable input from H. Blumenthal, for which we acknowledge our deep appreciation.

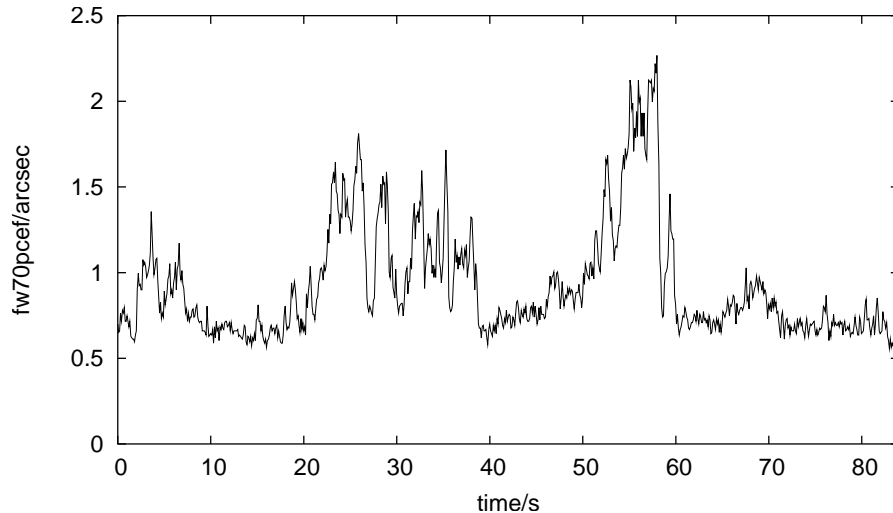


Figure 5. Example of rapid variations in the seeing from Baldwin *et al.*¹¹ (reproduced with permission of the authors). The y-coordinate, fw70pcef , is a measure of the intrinsic seeing in arcseconds which is accurate to about 10% at any instant. It can be seen that r_0 changes by a factor of more than 3 over very short timescales, with some changes occurring in less than a second.

REFERENCES

- [1] Shao, M. and Staelin, D. H., “First fringe measurements with a phase-tracking stellar interferometer,” *Appl. Opt.* **19**, 1519–1522 (1980).
- [2] Colavita, M. M., Wallace, J. K., Hines, B. E., Gursel, Y., Malbet, F., Palmer, D. L., Pan, X. P., Shao, M., Yu, J. W., Boden, A. F., Dumont, P. J., Gubler, J., Koresko, C. D., Kulkarni, S. R., Lane, B. F., Mobley, D. W., and van Belle, G. T., “The Palomar Testbed Interferometer,” *ApJ* **510**, 505–521 (1999).
- [3] ten Brummelaar, T. A., McAlister, H. A., Ridgway, S. T., Bagnuolo, Jr., W. G., Turner, N. H., Sturmman, L., Sturmman, J., Berger, D. H., Ogden, C. E., Cadman, R., Hartkopf, W. I., Hopper, C. H., and Shure, M. A., “First Results from the CHARA Array. II. A Description of the Instrument,” *ApJ* **628**, 453–465 (2005).
- [4] Colavita, M. M., Wizinowich, P. L., and Akeson, R. L., “Keck Interferometer status and plans,” *Proc. SPIE* (2004).
- [5] Glindemann, A., Algomedo, J., Amestica, R., Ballester, P., Bauvir, B., Bugueño, E., Correia, S., Delgado, F., Delplancke, F., Derie, F., Duhoux, P., di Folco, E., Gennai, A., Gilli, B., Giordano, P., Gitton, P., Guisard, S., Housen, N., Huxley, A., Kervella, P., Kiekebusch, M., Koehler, B., Lévêque, S., Longinotti, A., Ménardi, S., Morel, S., Paresce, F., Phan Duc, T., Richichi, A., Schöller, M., Tarenghi, M., Wallander, A., Wittkowski, M., and Wilhelm, R., “The VLTI - A Status Report,” *Ap&SS* **286**, 35–44 (2003).
- [6] Tubbs, R. N., “Seeing timescales for large-aperture optical/infrared interferometers from simulations,” *Proc. SPIE* **5491**, 1240–+ (2004).
- [7] Tubbs, R., “Effect of wavefront corrugations on fringe motion in an astronomical interferometer with spatial filters,” *Appl. Opt.* **44**, 6253–6257 (2005).
- [8] Keen, J. W., Buscher, D. F., and Warner, P. J., “Numerical simulations of pinhole and single-mode fibre spatial filters for optical interferometers,” *MNRAS* **326**, 1381–1386 (2001).
- [9] Shaklan, S. B. and Roddier, F., “Single-mode fiber optics in a long-baseline interferometer,” *Appl. Opt.* **26**, 2159–2163 (1987).
- [10] Buscher, D. F., “Optimising a ground-based optical interferometer for sensitivity at low light levels,” *M. Not. R. Astr. Soc.* **235**, 1203–1226 (1988).
- [11] Baldwin, J. E., Warner, P. J., and Mackay, C. D., “The point spread function in Lucky Imaging and variations in seeing on short timescales,” *A&A* **480**, 589–597 (2008).